Sonochemical Method for the Preparation of Bismuth Sulfide Nanorods

Hui Wang,[†] Jun-Jie Zhu,*[,†] Jian-Min Zhu,[‡] and Hong-Yuan Chen[†]

Laboratory of Mesoscopic Materials Science and State Key Laboratory of Coordination Chemistry, Department of Chemistry, and National Laboratory of Solid State Microstructures, Nanjing University, Nanjing, 210093, People's Republic of China

Received: September 12, 2001; In Final Form: December 17, 2001

Bismuth sulfide nanorods have been successfully prepared by a sonochemical method from an aqueous solution of bismuth nitrate and sodium thiosulfate in the presence of complexing agents. Bismuth sulfide nanorods with different diameters and lengths could be obtained by using different complexing agents including ethylenediaminetetraacetic acid, triethanolamine, and sodium tartrate. Bi_2S_3 nanorods have also been successfully prepared by choosing thioacetamide as the sulfur source. When 20% *N*,*N*-dimethylformamide was used as the solvent, higher yield was observed and smaller sizes of Bi_2S_3 nanorods were obtained. The products were characterized by powder X-ray diffraction, transmission electron microscopy, selected area electron diffraction, high-resolution transmission electron microscopy, IR spectroscopy, and X-ray photoelectron spectroscopy. Probable mechanisms for the sonochemical formation of Bi_2S_3 nanorods in aqueous solutions are proposed.

Introduction

There has been considerable interest in the preparation of semiconductor nanorods or nanofibers and the investigation of their properties in the past decade.[1−9] Control over both nanocrystalline morphology and the crystal size is a new challenge to synthetic chemists and materials scientists.[9] Main group metal sulfides, selenides, and tellurides such as $A_2^{V}B_3^{VI}$ (A = Sb, Bi, As; B = S, Se, Te) group compounds are useful semiconductors which have applications in television cameras with photoconducting targets, thermoelectric devices, and electronic and optoelectronic devices and in IR spectroscopy.[10] Bismuth sulfide (Bi_2S_3) is a semiconductive material. It has a lamellar structure whose direct band gap E_g is 1.3 eV[11] and is useful for photodiode arrays or photovoltaics.[12−14] Bi_2S_3 also belongs to a family of solid-state materials with applications in cooling technologies based on the Peltier effect.[15]

Conventionally, bismuth sulfide is prepared by direct element reaction in a quartz vessel at high temperature.[10,16] The chemical deposition methods have been applied to prepare Bi_2S_3 through a reaction of bismuth salt complexed by triethanolamine (TEA) or ethylenediaminetetraacetic acid (EDTA) in an aqueous solution containing a sulfur source such as thioacetamide (TAA), thiourea, sodium thiosulfate, or gaseous H_2S. The powders obtained through this route are mostly amorphous or poorly crystallized.[17−22] The chemical deposition of Bi_2S_3 in nonaqueous solution has also been reported.[23,24] Colloidal suspensions of bismuth sulfide have been prepared in water at room temperature with a solution of $Bi(NO_3)_3$ and $Na_2S{\cdot}9H_2O$ as the starting materials, but sodium hexametaphosphate is needed to stabilize Bi^{3+} and only colloidal particles can be obtained.[25] Crystallized bismuth sulfide has been prepared by thermal decomposition of various precursors such as bismuth dithiocarbamate complexes,[26] metal ethylxanthate,[27] bismuth−thiourea complex,[28] and thiosulfatobismuth.[29] However, high temperature is required and the final products contain some impurities. In recent years, Yu et al. conducted experiments in which Bi_2S_3 nanorods were successfully prepared and Bi(Se,S) nanowires were obtained by the hydrothermal or solvothermal technique.[30−32] The size and morphology of the products can be controlled by applying different reaction conditions including temperature, reaction time, and solvents. However, this method requires relatively high pressure, and it takes a long time for the reaction to be completed. Monteiro et al. also reported a novel single-source method for the preparation of Bi_2S_3 nanofibers.[33] However, the presursor compound $Bi\{S_2CN(CH_3)(C_6H_{13})\}_3$ must be prepared first.

Ultrasound has become an important tool in chemistry in recent years. It has been extensively used to generate novel materials with unusual properties, because it causes the formation of particles with a much smaller size and higher surface area than those reported by other methods. When solutions are exposed to strong ultrasound irradiation, bubbles are implosively collapsed by acoustic fields in the solution. High-temperature and high-pressure fields are produced at the centers of the bubbles. This effect is known as acoustic cavitation. The temperature is estimated to be 5000 K, the pressure reaches over 1800 atm,[34] and the cooling rate is over 10^{10} K/s when the bubbles implode, which enables many chemical reactions to occur. Ultrasound offers a very attractive method for the preparation of nanosized materials. It has shown very rapid growth in its application to materials science due to its unique reaction effects. The advantages of this method include a rapid reaction rate, the controllable reaction conditions, and the ability to form nanoparticles with uniform shapes, narrow size distributions, and high purities. The sonochemical method has been successfully applied to the preparation of various nanosized materials including metals,[34−37] metal carbides,[38] metal oxides[39−42] and metal chalcogenides[43−46] et al.

* Corresponding author. Fax: +86-25-3317761. E-mail: gxyz@nju.edu.cn.
[†] Department of Chemistry.
[‡] National Laboratory of Solid State Microstructures.

10.1021/jp0135003 CCC: $22.00
Published on Web 03/23/2002

TABLE 1: Preparation Conditions and Corresponding Results[a]

starting materials	solvent	mean dimens obsd from TEM/nm	yield/%
25 mM $Bi(NO_3)_3$, 50 mM TEA, 100 mM $Na_2S_2O_3$	H_2O	25 × 220	60
25 mM $Bi(NO_3)_3$, 50 mM TEA, 30 mM TAA	H_2O	20 × 80	60
25 mM $Bi(NO_3)_3$, 50 mM EDTA, 100 mM $Na_2S_2O_3$	H_2O	15 × 100	30
25 mM $Bi(NO_3)_3$, 50 mM sodium tartrate, 100 mM $Na_2S_2O_3$	H_2O	20 × 60	50
25 mM $Bi(NO_3)_3$, 50 mM TEA, 100 mM $Na_2S_2O_3$	20% DMF−H_2O	6 × 30	90

[a] In all of these experiments, the reaction time is 2 h and the total volume of the stock solutions is 100 mL.

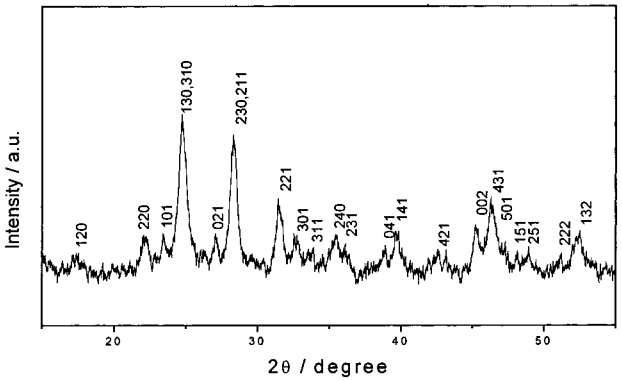

Figure 1. Powder XRD pattern of the as-prepared Bi_2S_3 nanorods.

Herein, we report a novel sonochemical method for the preparation of bismuth sulfide nanorods in an aqueous solution containing bismuth nitrate and sodium thiosulfate or thioacetamide in the presence of complexing agents such as EDTA, TEA, and sodium tartrate. To the best of our knowledge, preparation of nanocrystalline V−VI group semiconductors by sonochemical method has never been reported before. The products were characterized by using techniques such as powder X-ray diffraction (XRD), transmission electron microscopy (TEM), selected area electron diffraction (SAED), high-resolution transmission electron microscopy (HRTEM), IR spectroscopy, and X-ray photoelectron spectroscopy (XPS). It is found to be a fast, convenient, mild, energy efficient, and environmentally friendly route for producing Bi_2S_3 nanorods in only one step.

Experimental Section

All the reagents used in our experiments were of analytical purity and were used without further purificaiton. $Bi(NO_3)_3 \cdot 5H_2O$ was purchased from Beijing (China) chemical reagents factory. Sodium tartrate and sodium thiosulfate were purchased from Shanghai (China) chemical reagents factory. EDTA, TEA, TAA, and *N*,*N*-dimethylformamide (DMF) were purchased from Nanjing (China) chemical reagents factory.

In a typical procedure, $Bi(NO_3)_3 \cdot 5H_2O$, TEA, and $Na_2S_2O_3$ were introduced into distilled water to give the final concentrations of 25 mM $Bi(NO_3)_3$, 50 mM TEA, and 100 mM $Na_2S_2O_3$, and the total volume of the solution was 100 mL (Table 1). Then the mixture solution was exposed to high-intensity ultrasound irradiation under ambient air for 120 min. Ultrasound irradiation was accomplished with a high-intensity ultrasonic probe (Xinzhi Co.; 0.6 cm diameter; Ti-horn, 20 kHz, 60W/cm^2) immersed directly in the reaction solution. The sonication was conducted without cooling so that a temperature of 343 K was reached at the end of the reaction. When the reaction was finished, black precipitates were obtained. After being cooled to room temperature, the precipitates were centrifuged, washed with 0.1 M HCl, distilled water, absolute ethanol, and acetone in sequence, and dried in air at room temperature. The final products were collected for characterization. The products were characterized by powder XRD, TEM, SAED, HRTEM, IR spectroscopy, and XPS.

Powder XRD measurements were performed on a Shimadzu XD-3A X-ray diffractometer at a scanning rate of 4°/min in the 2θ range from 15 to 60°,with graphite monochromatized Cu Kα radiation (λ = 0.154 18 nm) and nickel filter. TEM images and SAED pictures were recorded on a JEOL-JEM 200CX transmission electron microscope, using an accelerating voltage of 200 kV. The samples used for TEM observations were prepared by dispersing some products in ethanol followed by ultrasonic vibration for 30 min and then placing a drop of the dispersion onto a copper grid coated with a layer of amorphous carbon. HRTEM images were obtained by employing a JEOL-4000EX high-resolution transmission electron microscope with a 400 kV accelerating voltage. Further evidence for the purity of Bi_2S_3 was obtained by the XPS of the product. The XPS patterns were recorded on an ESCALAB MK II X-ray

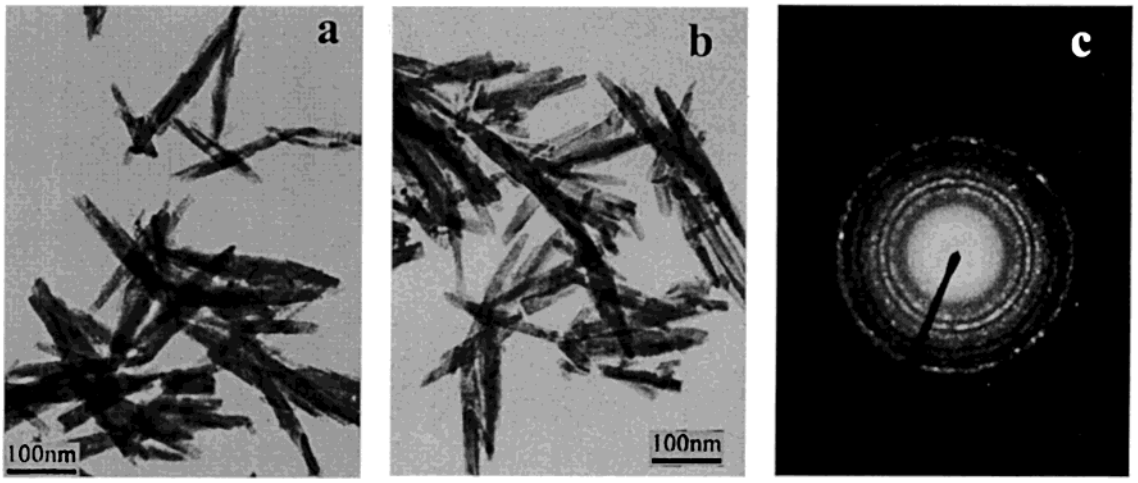

Figure 2. (a, b) TEM images of the as-prepared Bi_2S_3 nanorods selected in different areas; (c) SEAD image of the as-prepared Bi_2S_3 nanorods.

Figure 3. HRTEM image of the as-prepared Bi_2S_3 nanorods (bar = 20 nm).

photoelectron spectrometer by using nonmonochromatized Mg Kα X-ray as the excitation source and choosing C1s (284.6 eV) as the reference line. IR spectroscopy was carried out on a Bruker Ifs66 Fourier transform infrared (FT-IR) spectrometer (Bruker Co.) in the single-beam mode over the range of 500-4000 cm^{-1} at room temperature.

Results

XRD Studies. The powder XRD pattern of the product is shown in Figure 1. All the diffraction peaks can be indexed to be a pure orthorhombic phase for Bi_2S_3 with cell constants a = 1.1130 nm, b = 1.1250 nm, and c = 0.3971 nm. The intensities and positions of the peaks are in good agreement with literature

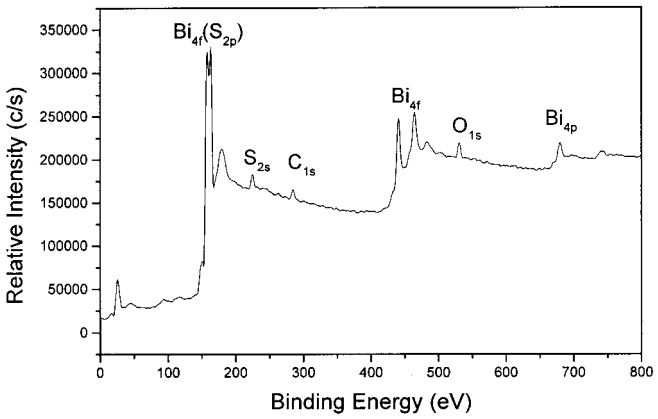

Figure 4. Wide XPS picture of the as-prepared Bi_2S_3 nanorods.

values.[47] No peaks of any other phases are detected, indicating the high purity of the product.

TEM, HRTEM, and SAED Analyses. The size and morphology of the product is analyzed by TEM. The TEM images (Figure 2a,b) reveal that the product consists of needle-shaped nanorods. The diameter of the nanorods is in the range from 20 to 30 nm, and the length is about 200−250 nm. The observed rod type morphology of the product is possibly due to the inherent chain type structure of bismuth sulfide.[10] It is known that Bi_2S_3 crystallizes with a lamellar structure with linked Bi_2S_3 units forming infinite bands, which in turn are connected via weaker van der Waals interactions.[11] It seems that the formation of Bi_2S_3 may have been originated from the preferential directional growth of Bi_2S_3 crystallites.

The crystallinity and crystallography of the product are proven by SAED. Transmission electron diffraction performed in a set of such nanorods leads to a pattern as shown in Figure 2c. The ED measurements show that the particles are well-crystallized and the diffraction rings match the XRD peaks very well.

A HRTEM image recorded on an individual nanorod provides further insight into their structures. The HRTEM image of a single Bi_2S_3 nanorod (Figure 3) exhibits good crystalline and clear lattice fringes. The interplanar spacing is about 0.398 nm, which corresponds to the *c* axis of the orthorhombic structure of Bi_2S_3. These lattice fringes are parallel to the rod axis of Bi_2S_3 nanorods.

XPS Studies. The product was also characterized by XPS for evaluation of its composition and purity. The wide-scan XPS spectrum of the product is shown in Figure 4. The binding energies obtained in the XPS analysis are standerized for specimen charging using C1s as the reference at 284.6 eV. No peaks of other elements except C, O, Bi, and S are observed on the picture. The peaks for O can be attributed to the O_2, CO_2, or H_2O absorbing on the surface of the sample. The absorbed O_2, CO_2, or H_2O are common to powder samples that have been exposed to the atmosphere and are more pronounced for ultrafine powders with high surface area.

The high-resolution XPS spectra of the as-prepared Bi_2S_3 nanorods are shown in Figure 5. The two strong peaks taken for the Bi region at 166.5 and 172.4 eV are assigned to the Bi (4f) binding energy. The peak measured in the S energy region detected at 225.0 eV is attributed to the S (2s) transition. The peak areas of Bi (4f) and S (2s) are measured, and quantification of the peaks gives the atomic ratio of Bi:S to be approximately 2:3.

FT-IR Spectroscopy. Figure 6 shows the FT-IR spectrum collected on the Bi_2S_3 powders mulled in KBr wafer. No peaks

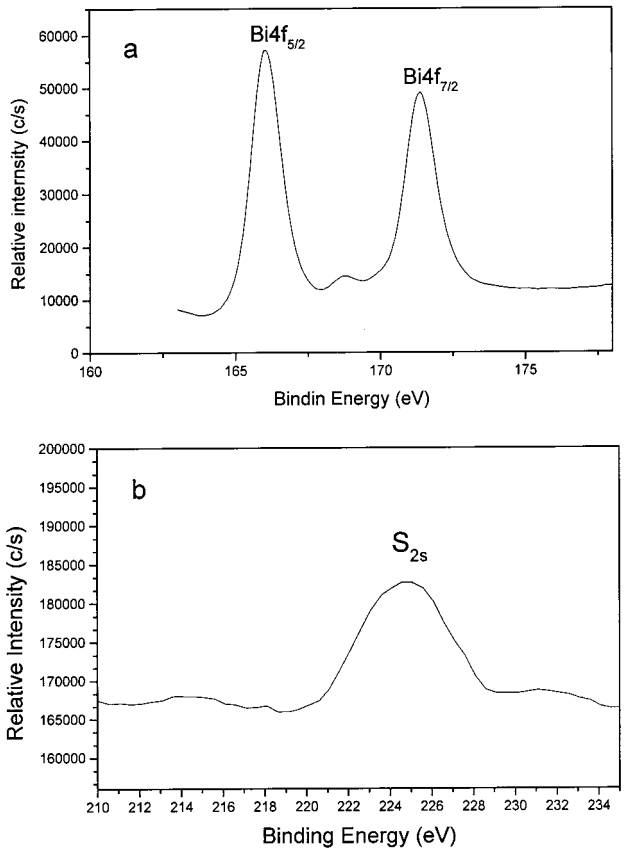

Figure 5. High-resolution XPS spectra of Bi_2S_3: (a) Bi4f; (b) S2s.

of Bi_2O_3 are detected in the IR spectrum. The broad absorption peak from 3650 to 3000 cm^{-1} corresponds to the −OH group of H_2O, indicating the existence of water absorbed on the surface of the product. The peak centered at approximately 1625 cm^{-1} belongs to the C═O stretching mode of the absorbed CO_2. The absorbed H_2O and CO_2 on the surface of Bi_2S_3 ultrafine powders prepared by hydrothermal or solvothermal method have also been reported previously.[30,31] The two peaks located at 1185.33 and 1110.98 cm^{-1} correspond to the C−O bond, and two weak peaks at about 2924.13 and 2885.15 cm^{-1} as well as a set of weak peaks ranging from 1360 to 1520 cm^{-1} can be assigned to the C−H bond of the $-CH_3$ and $-CH_2-$ groups. This may be indicative of the existence of CH_3CH_2OH absorbed on the product surface. These absorbed CH_3CH_2OH may come from the washing process.

Discussion

Ultrasound waves that are intense enough to produce cavitation can drive chemical reactions such as oxidation, reduction, dissolution, and decomposition.[48,49] Other reactions driven by high-intensity ultrasound irradiation, such as promotion of polymerization, have also been reported. It has been known that during an aqueous sonochemical process, the elevated temperatures and pressures inside the collapsing bubbles cause water to vaporize and further pyrolyze into $H^{\cdot}$ and $OH^{\cdot}$ radicals. The mechanism of the sonochemical formation of Bi_2S_3 nanorods is probably related to the radical species generated from water molecules by the absorption of the ultrasound energy. The probable reaction process for the sonochemical formation of Bi_2S_3 nanorods in aqueous solution can be summarized as follows:

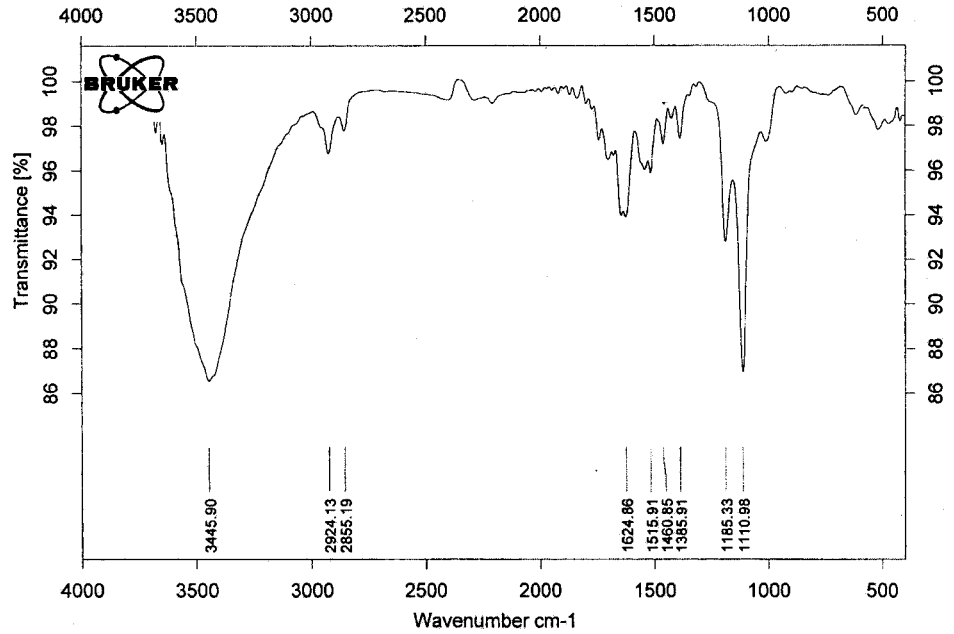

Figure 6. FT-IR spectrum of the as-prepared Bi_2S_3 nanorods.

$$Bi(TEA)_x^{3+} \rightleftharpoons Bi^{3+} + xTEA \quad (1)$$

$$H_2O))))) H^{\cdot} + OH^{\cdot} \quad (2)$$

$$2H^{\cdot} + S_2O_3^{2-} \rightarrow S^{2-} + 2H^{+} + SO_3^{2-} \quad (3)$$

$$2Bi^{3+} + 3S^{2-} \rightarrow Bi_2S_3 \quad (4)$$

$$nBi_2S_3 \rightarrow (Bi_2S_3)_n \quad (5)$$

Initially, the complexing actions between Bi^{3+} and TEA lead to the formation of Bi−TEA complexes. Reaction 2 represents the formation of primary radicals by the ultrasound-initiated dissociation of water within the collapsing gas bubbles. Reactions 3−5 represent the main steps leading to the formation of Bi_2S_3 nanorods. The in-situ generated $H^{\cdot}$ is a highly reducing radical and can react with $S_2O_3^{2-}$ ions rapidly via reaction 3 to form S^{2-} ions. Then S^{2-} ions combine with Bi^{3+} ions which are released from the Bi−TEA complexes to yield Bi_2S_3 nuclei. It is observed that after sonication for about 20 min, the mixture solution turned light brown and turbid, indicating the formation of Bi_2S_3 nuclei. These freshly formed nuclei in the solution are unstable and have the tendency to grow into larger particles. Once the nuclei are formed, there are a large number of dangling bonds, defects, or traps on the nuclei surfaces.[50] During the sonication time, the surface state might change. The dangling bonds, defects, or traps will decrease gradually, and the particles will grow until the surface state becomes stable and the size of the particles ceases to increase any more. During the crystal growth process, Bi_2S_3 presents a preferential directional growth due to its inherent chain-type structure. As a result, the product presents rod type morphology. We observed that after the formation of Bi_2S_3 nuclei, the color of the reactants mixture turns darker gradually and finally results in a black turbidity after 90 min of sonication, indicating the formation of the final product. The gradual change in color may be indicative of the growth process of Bi_2S_3 nanorods.

To make a comparison, we have carried out experiments in the absence of the inducement of ultrasound irradiation at both 343K and room temperature. When such a reaction was carried out with electromagnetic stir at 343 K for 2 h, the Bi_2S_3 powder

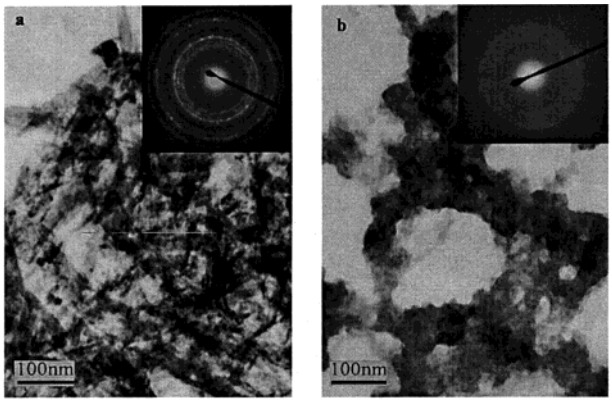

Figure 7. TEM images and SAED pictures of the products prepared in the absence of ultrasound irradiation: (a) at 343 K for 2 h and (b) at room temperature for 60 h.

obtained was poorly crystalline and consisted of irregular nanorods in an aggregated state (Figure 7a). If this reaction was carried out at room temperature, the reaction rate became much slower and it took over 60 h for the reaction to be completed. The final precipitate obtained after 60 h was found to be amorphous according to the ED picture and the XRD pattern. In the TEM image (Figure 7b), no rodlike particles are observed. The particles are irregular in shape and highly agglomerated, and it is therefore difficult to measure the individual particle size. These results show that ultrasound irradiation is favorable for the formation of well-dispersed $Bi2_2S_3$ nanorods with uniform shape and high crystallinity.

We also managed to prepare Bi_2S_3 naorods by choosing TAA as the sulfur source. If 100 mM $Na_2S_2O_3$ was replaced by 30 mM TAA and all the other preparation conditions remain unchanged, thinner and shorter Bi_2S_3 nanorods were obtained. The mean dimensions of the as-prepared Bi_2S_3 nanorods are 20 × 80 nm, as can be observed in the TEM image (Figure 8a). In this case, the likely steps and explanation for the sonochemical reduction process can be explained as follows: The cleavage of water could be linked with the addition across the C═S bond to give $CH_3C(NH_2)(OH)-SH$. Repeating this process would then result in the formation of $CH_3C(NH_2)(OH)_2$ (which would immediately lose water to give CH_3CONH_2) and

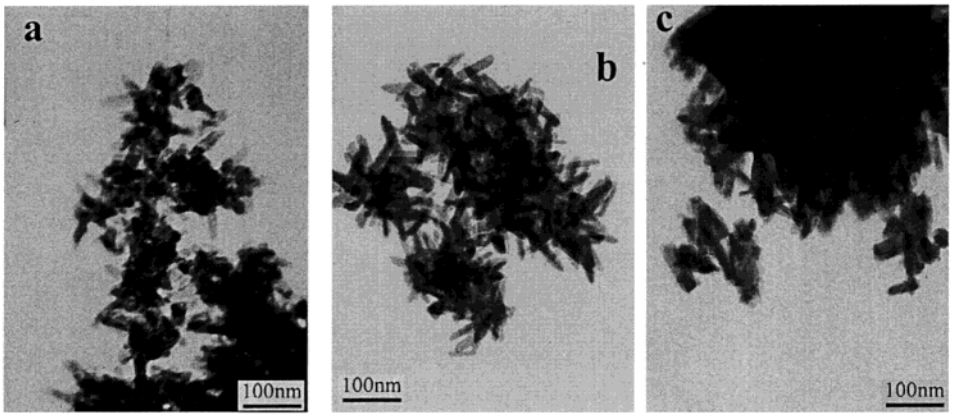

Figure 8. TEM images of Bi_2S_3 nanorods: (a) from the preparation using TAA as the sulfur source; (b) in the presence of EDTA; (c) in the presence of sodium tartrate.

H_2S. Then the released H_2S reacts with Bi^{3+} to yield Bi_2S_3.

$$H_2O))))))\ H^{\cdot} + OH^{\cdot} \quad (6)$$

$$H^{\cdot} + OH^{\cdot} + CH_3CSNH_2 \rightarrow CH_3C(NH_2)(OH)-SH \quad (7)$$

$$H^{\cdot} + OH^{\cdot} + CH_3C(NH_2)(OH)-SH \rightarrow CH_3C(NH_2)(OH)_2 + H_2S \quad (8)$$

$$CH_3C(NH_2)(OH)_2 \rightarrow CH_3CO(NH_2) + H_2O \quad (9)$$

$$2Bi^{3+} + 3H_2S \rightarrow Bi_2S_3 + 6H^+ \quad (10)$$

$$nBi_2S_3 \rightarrow (Bi_2S_3)_n \quad (11)$$

The formation of H_2S may follow another route as well. It may be related to the ultrasound-induced reduction of CH_3CSNH_2. The main steps can be explained as follows:

$$H_2O))))))\ H^{\cdot} + OH^{\cdot} \quad (12)$$

$$2H^{\cdot} + CH_3CSNH_2 \rightarrow H_2S + {}^{\cdot}C(NH_2)CH_3 \quad (13)$$

In this case, the as-prepared Bi_2S_3 nanorods have a smaller diameter and length. It may probably be attributed to the larger nucleation rate of Bi_2S_3 when TAA was used as the sulfer source instead of $Na_2S_2O_3$.

The complexing agents play an important role in the formation of Bi_2S_3 nanorods. The presence of complexing agents has influence on both the nucleation rate and growth rate of Bi_2S_3, which leads to the formation of Bi_2S_3 nanorods with different diameters and lengths. We have also carried out the experiment using EDTA as the complexing agent. In this case, the product consists of aggregated nanorods with an average diameter of 15 nm and a length of 100 nm, as can be observed in Figure 8b. If the Bi_2S_3 nanorods are prepared in the presence of sodium tartrate, they become even shorter and more aggregated (Figure 8c). The mean dimensions of the as-prepared Bi_2S_3 nanorods are 20 × 60 nm.

It has been known that during the sonochemical process, three different regions[49] are formed: (a) the inner environment (gas phase) of the collapsing bubbles, where the elevated temperatures and pressures are produced, leading to the formation of $H^{\cdot}$ and $OH^{\cdot}$ radicals; (b) the interfacial region between the cavitation bubbles and the bulk solution where the temperature is lower than in the gas-phase region but still high enough to induce a sonochemical reaction; (c) the bulk solution, which is at ambient temperature. Among the three regions mentioned above, it appears that the current sonochemical reaction occurs within the interfacial region, yielding nanoparticles, because of the very high quenching rate experienced by the products. In the bulk solution, factors favoring maximum acoustic cavitation and sonochemical yields are low viscosity, high surface tension, low vapor pressure, and high sound speed. DMF is favorable for the sonochemical process for it fulfills all of the criteria mentioned above. When we use a 20% DMF−water solution as the solvent, a better yield is obtained. The DMF accumulated at the interfacial region[51] is likely to out-compete the concurrent process of the removal of $OH^{\cdot}$ radicals via

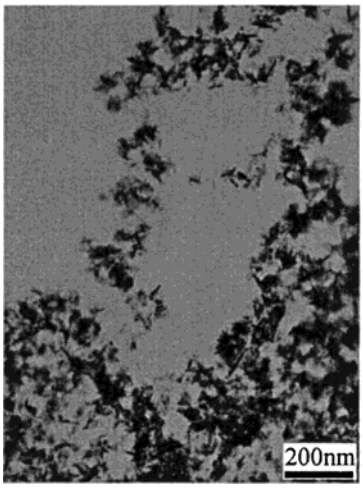

Figure 9. TEM image of the Bi_2S_3 nanorods prepared in 20% DMF−water.

$$OH^{\cdot} + (CH_3)_2NCHO \rightarrow {}^{\cdot}CH_2N(CH_3)CHO + H_2O \quad (14)$$

This is one of the most likely factors responsible for the continuing increase of the sonochemical radical yields. So when the 20% DMF−water solution is used as the solvent instead of water alone, the sonochemical process is enhanced, which leads to better yields of the product. Furthermore, the existence of DMF in aqueous solution influences the size and morphology of the product. When the 20% DMF−water solution is used as the solvent, the size of the Bi_2S_3 nanorods obtained becomes smaller. As observed in Figure 9, the mean dimensions of the Bi_2S_3 nanorods are 6 × 30 nm. The decrease in size may be attributed to the faster nucleation rate caused by the enhancement of the sonochemical process.

Conclusion

In summary, a novel sonochemical method for the preparation of Bi_2S_3 nanorods has been reported for the first time. Bi_2S_3 nanorods can be successfully prepared via a sonochemical route from an aqueous solution of bismuth nitrate and sodium sodium thiosulfate (or TAA) in the presence of complexating agents. It is a convenient, mild, efficient and environmentally friendly route for preparing Bi_2S_3 nanorods. It may be predicted that upscaling of this method will lead to large quantities of nanosized Bi_2S_3 rods. It can also be extended to the preparation of some other sulfide semiconductors.

Acknowledgment. This work is supported by the National Natural Science Foundation of China (Grants No. 50072006 and No. 20075010) and the Jiangsu Science and Technology Foundation (Grant BG 2001039). The authors thank Ms. Xiaoning Zhao and Ms. Xiaoshu Wang, Modern Analytic Center of Nanjing University, for extending their facilities to us. We are also grateful to Mr. Tao Ding and Mr. Xiaofeng Qiu for their kind assistance.

References and Notes

(1) Morales, A. M.; Lieber, C. M. *Science* **1998**, *279*, 208.
(2) Han, W. Q.; Fan, S. S.; Li, Q. Q.; Hu, Y. D. *Science* **1997**, *277*, 1287.
(3) Alivisatos, A. P. *Science* **1996**, *271*, 933.
(4) Braun, P. V.; Osenar, P.; Stupp, S. I. *Nature* **1996**, *380*, 325.
(5) Trentler, T. J.; Hickman, K. M.; Goel, S. C.; Viano, A. M.; Gibbons, P. C.; Buhro, W. E. *Science* **1995**, *270*, 1791.
(6) Trentler, T. J.; Goel, S. C.; Hickman, K. M.; Viano, A. M.; Chiang, M. Y.; Beatty, A. M.; Gibbons, P. C.; Buhro, W. E. *J. Am. Chem. Soc.* **1997**, *119*, 2172.
(7) Yang, J. P.; Meldrum, F. C.; Fendler, J. H. *J. Phys. Chem.* **1995**, *99*, 5500.
(8) Klein, J. D.; Herrick, R. D.; Palmer, D.; Sailor, M. J. *Chem. Mater.* **1993**, *5*, 902.
(9) Shiang, J. J.; Kadavanich, A. V.; Grubbs, R. K.; Alivisatos, A. P. *J. Phys. Chem.* **1995**, *99*, 17417.
(10) Arivuoli, D.; Gnanam, F. D.; Ramasamy, P. *J. Mater. Sci. Lett.* **1988**, *7*, 711.
(11) Black, J.; Conwell, E. M.; Seigle, L.; Spencer, C. W. *J. Phys. Chem. Solids* **1957**, *2*, 240.
(12) Nayak, B. B.; Acharya, H. N.; Mitra, G. B.; Mathur, B. K. *Thin Solid Films* **1983**, *105*, 17.
(13) Pawar, S. H.; Bhosale, P. N.; Uplane, M. D.; Tanhankar, S. *Thin Solid Films* **1983**, *110*, 165.
(14) Farrugia, L. J.; Lawlot, F. J.; Norman, N. C. *Polyhedron* **1995**, *14*, 311.
(15) Boudjouk, P.; Remington, M. P.; Grier, D. G.; Jarabek, B. R.; McCarthy, G. J. *Inorg. Chem.* **1998**, *37*, 3538.
(16) Kaito, C.; Saito, Y.; Fujita, K. *J. Cryst. Growth* **1989**, *94*, 967.
(17) Biswas, S.; Mondal, A.; Mukherjee, D.; Pramanik, P. *J. Electrochem. Soc.* **1986**, *133*, 48.
(18) Pramanik, P.; Bhattachrya, S. *J. Mater. Sci. Lett.* **1987**, *6*, 1105.
(19) Lokhande, C. D.; Yermune, V. S.; Pawar, S. H. *J. Electrochem. Soc.* **1988**, *135*, 1852.
(20) Engelken, R. D.; Ali, S.; Chang, L. N.; Brinkley, C.; Turner, K.; Hester, C. *Mater. Lett.* **1990**, *10*, 264.
(21) Yesugade, N. S.; Lokhande, C. D.; Bhosale, C. H. *Thin Solid Films* **1995**, *263*, 145.
(22) Desai, J. D.; Lokhande, C. D. *Indian J. Pure Appl. Phys.* **1993**, *31*, 152.
(23) Baranski, A. S.; Fawcett, W. R. *J. Electrochem. Soc.* **1980**, *127*, 766.
(24) Desai, J. D.; Lokhande, C. D. *Mater. Chem. Phys.* **1993**, *34*, 313.
(25) Variano, B. F.; Hwang, D. M.; Sandroff, C. S.; Wiltzius, P.; Jing, T. W.; Ong, N. P. *J. Phys. Chem.* **1987**, *91*, 6455.
(26) Nomura, R.; Kanaya, K.; Matsuda, H. *Bull. Chem. Soc. Jpn.* **1989**, *62*, 939.
(27) Larionov, S. V.; Patrina, L. A.; Uskov, E. M. *Izv. Sib. Otd. Akad. Nauk SSSR, Ser. Khim. Nauk* **1979**, *3*, 94.
(28) Popov, V. N.; Kolodezev, A. B.; Safonov, V. P. *Tezisy Dokl. Vses. Soveshch: Tekhnol., protsessy, Appar. Kach. Prom. Lyuminoforov* **1977**, 98.
(29) Cyganski, A.; Kobylecka, J. *Thermochim. Acta* **1981**, *45*, 65.
(30) Yu, S. H.; Yang, J.; Wu, Y. S.; Han, Z. H.; Xie, Y.; Qian, Y. T. *Mater. Res. Bull.* **1998**, *33*, 1661.
(31) Yu, S. H.; Qian, Y. T.; Shu, L.; Xie, Y.; Yang, J.; Wang, C. S. *Mater. Lett.* **1998**, *35*, 116.
(32) Yu, S. H.; Shu, L.; Yang, J.; Han, Z. H.; Qian, Y. T.; Zhang, Y. H. *J. Mater. Res.* **1999**, *14*, 4157.
(33) Monteiro, O. C.; Triodade, T. *J. Mater. Sci. Lett.* **2000**, *19*, 859.
(34) Suslick, K. S.; Choe, S. B.; Cichowlas, A. A.; Grinstaff, M. W. *Nature* **1991**, *353*, 414.
(35) Koltypin, Yu.; Katabi, G.; Prozorov, R.; Gedanken, A. *J. Non-Cryst. Solids* **1996**, *201*, 159.
(36) Nagata, Y.; Mizukoshi, Y.; Okitsu, K.; Maeda, Y. *Radiat. Res.* **1996**, *146*, 333.
(37) Okitsu, K.; Mizukoshi, Y.; Bandow, H.; Maeda, Y.; Yamamoto, T.; Nagata, Y. *Ultrason. Sonochem.* **1996**, *3*, 249.
(38) Hyeon, T.; Fang, M.; Suslick, K. S. *J. Am. Chem. Soc.* **1996**, *118*, 5492.
(39) Cao, X.; Koltypin, Yu.; Katabi, G.; Felner, I.; Gedanken, A. *J. Mater. Res.* **1997**, *12*, 405.
(40) Arul Dhas, N.; Gedanken, A. *J. Phys. Chem. B* **1997**, *101*, 9495.
(41) Vijaya Kumar, R.; Diamant, Y.; Gedanken, A. *Chem. Mater.* **2000**, *12*, 2301.
(42) Patra, A.; Sominska, E.; Ramesh, S.; Koltypin, Yu.; Zhong, Z.; Minti, H.; Reisfeld, R.; Gedanken, A. *J. Phys. Chem. B* **1999**, *103*, 3361.
(43) Zhu, J. J.; Koltypin, Yu.; Gedanken, A. *Chem. Mater.* **2000**, *12*, 73.
(44) Li, B.; Xie, Y.; Huang, J. X.; Liu, Y.; Qian, Y. T. *Chem. Mater.* **2000**, *12*, 2614.
(45) Mdleleni, M. M.; Hyeon, T.; Suslick, K. S. *J. Am. Chem. Soc.* **1998**, *120*, 6189.
(46) Wang, G. Z.; Wang, Y. W.; Chen, W.; Liang, C. H.; Li, G. H.; Zhang, L. D. *Mater. Lett.* **2001**, *48*, 269.
(47) *JCPDS* File No. 17-320.
(48) Suslick, K. S. *Ultrasound: Its Chemical, Physical and Biological Effects;* VCH: Weinhein, Germany, 1988.
(49) Suslick, K. S.; Hammerton, D. A.; Cline, R. E. *J. Am. Chem. Soc.* **1986**, *108*, 5641.
(50) Chen, W.; Wang, Z.; Lin, Z.; Lin, L. *J. Appl. Phys.* **1997**, *82*, 3111.
(51) Misik, V.; Kirschenbaum, L. J.; Riesz, P. *J. Phys. Chem.* **1995**, *99*, 5970.